Spectral Imaging with Dual Energy CT
Comparison of different technologies and workflows

Sebastian Faby, PhD
Juergen Merz, PhD
Bernhard Krauss, PhD
Florian Kuemmel, PhD
Computed Tomography, Siemens Healthcare GmbH
Forchheim, Germany

International version.
Not for distribution or use in the U.S.

siemens.com/ct

SIEMENS
Healthineers

....

Contents

....

1. Introduction to Dual Energy CT

Although dual energy CT (DECT) has only gained broader attention in the last years, the idea already dates back to the beginning of CT. The first clinical CT scan was done in 1971 on Hounsfield's EMI head scanner and in 1975 the Siemens SIRETOM was introduced. Already in 1976 Alvarez and Macovski published a paper on "Energy-selective reconstructions in X-ray computerized tomography" [1], followed by Brook's publication from 1977 on "A quantitative theory of the Hounsfield unit and its application to dual energy scanning" [2]. In the energy range used for CT, the X-ray absorption is governed by two physical processes: the photoelectric effect and Compton scattering, with the contributions of the two processes varying by material and X-ray energy. Due to this variation of the energy dependence of X-ray absorption for different materials, scanning with two different energies provides the required information for material differentiation, see Fig. 1. Although the X-ray spectra in CT are not monoenergetic, the average energy of the spectra is different for different tube voltages. Scanning a patient with two different tube voltages can thus provide the required energy information. Clinical benefits may result from the material characterization, going beyond simple morphology. For example, in conventional single energy CT the CT value of a bony structure and a vessel with iodinated contrast agent may be the same, however, DECT allows to differentiate bone from iodine, which can be used for a bone removal to provide a clear view at vessels in CTA studies.
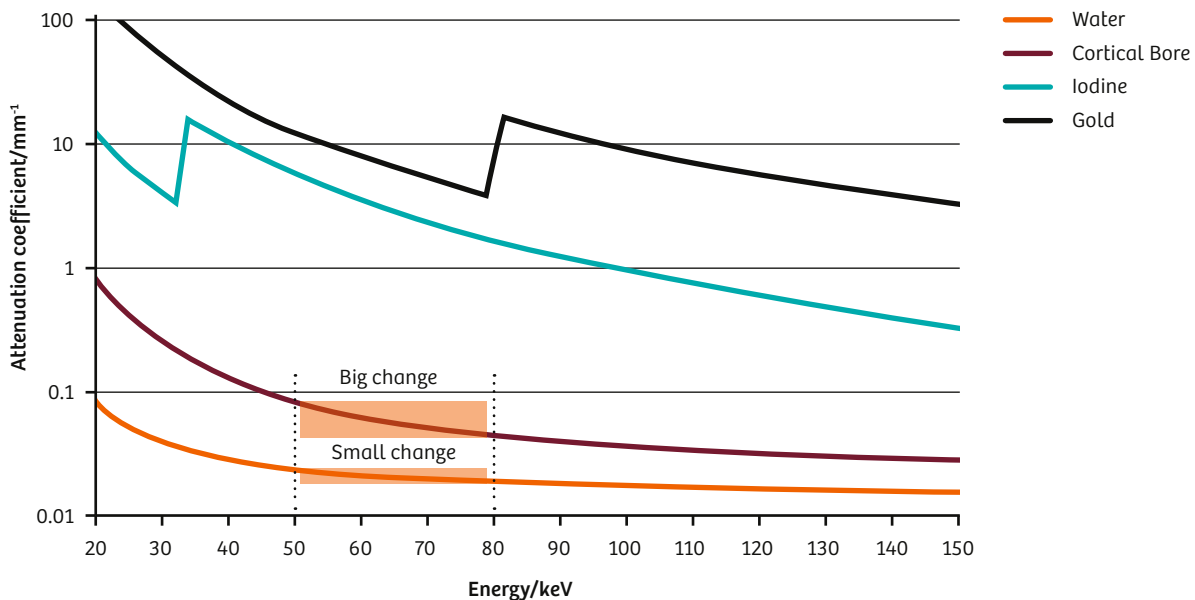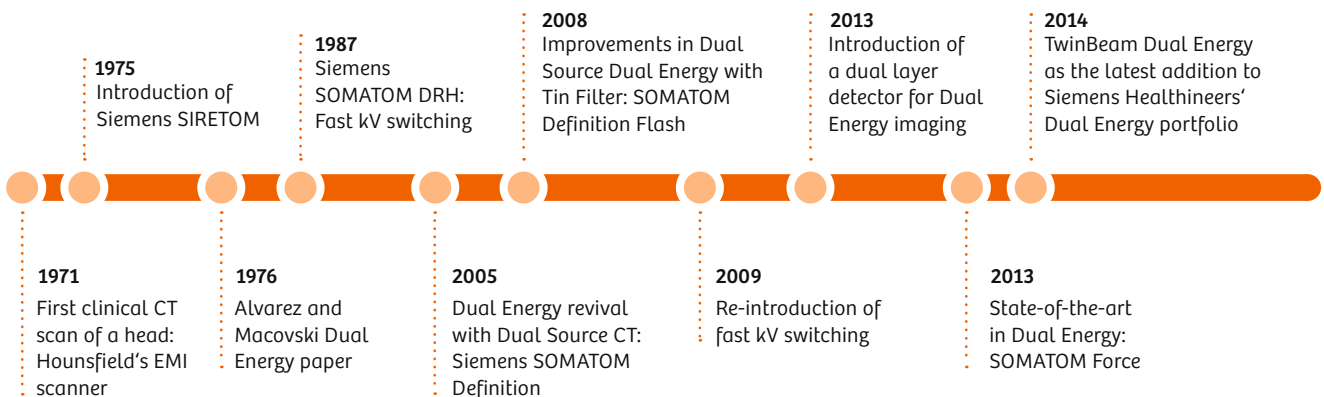

Fig. 1: Energy dependence of the attenuation coefficient of different materials. The different change in attenuation at two different energies is illustrated for water and bone. Please note the K-edges of iodine and gold.

2. History of DECT and available solutions

As mentioned above, the idea of DECT came up already in the 1970s and the first available commercial DECT scanner was the Siemens SOMATOM DRH in 1987 [3]. It used a fast kV switching technique where the tube voltage was alternated between 85 kV and 125 kV from projection to projection. The main application back then was bone mineral density analysis. This approach was abandoned due to patient dose penalties (i.e. until today this approach does not enable a dose modulated scan) and other inherent drawbacks of this approach as well as the fact that DE X-ray absorptiometry was already available as an alternative for this clinical question. In 2005 DECT experienced a revival with the introduction of the first Dual Source CT (Siemens SOMATOM Definition) [4]. Two source-detector systems are mounted in the same imaging plane at an angle of 90°. These two X-ray tubes can simultaneously be operated at different tube voltages (80 kV/140 kV). An improved Dual Source CT was introduced in 2008 (Siemens SOMATOM Definition Flash) featuring an additional tin filter (Sn) at one of the X-ray tubes to improve the spectral separation by removing low energy photons from the high energy spectrum (Sn140 kV) [5]. In 2009, fast kV switching from the 1980s was re-introduced, this time by a different vendor (GE Discovery CT750 HD); switching between 80 kV and 140 kV from projection to projection [6]. Technical limitations prevent a fast tube current modulation between the 80 kV and 140 kV projections, leading to the problem of not enough tube output at 80 kV and too much output at 140 kV, which requires a 2:1 sampling scheme of low and high energy projection to at least partly compensate for this [7]–[8]. In 2013 another approach to DECT was introduced to the market: a CT scanner equipped with a dual layer detector (Philips IQon Spectral CT) [9]. In this case the first detector layer absorbs the low energy part of the spectrum while the second layer absorbs the high energy part to generate dual energy (DE) data sets, resulting in an increased spectral overlap due to the statistical nature of photon absorption. Dual Source DECT was further refined in 2013 for a better spectral separation enabled by an extended tube voltage range (70 kV to 150 kV) and a tin filter with increased thickness to remove even more low energy photons from the high energy spectrum with the release of SOMATOM Force [10]. The latest addition to the family of commercial DECT technologies was introduced in 2014 as TwinBeam Dual Energy, employing a split filter at the X-ray tube [11]–[12].

Fig. 2: The history of dual energy CT. Siemens Healthineers was the first to introduce DECT commercially and also the first to re-introduce it with Dual Source CT.

1975
Introduction of Siemens SIRETOM

1987
Siemens SOMATOM DRH: Fast kV switching

2008
Improvements in Dual Source Dual Energy with Tin Filter: SOMATOM Definition Flash

2013
Introduction of a dual layer detector for Dual Energy imaging

2014
TwinBeam Dual Energy as the latest addition to Siemens Healthineers' Dual Energy portfolio

1971
First clinical CT scan of a head: Hounsfield's EMI scanner

1976
Alvarez and Macovski Dual Energy paper

2005
Dual Energy revival with Dual Source CT: Siemens SOMATOM Definition

2009
Re-introduction of fast kV switching

2013
State-of-the-art in Dual Energy: SOMATOM Force

The two different materials positioned in z-direction of this split filter shift one part of the X-ray spectrum to lower and the other part to higher energies. Apart from these dedicated technical solutions for dual energy imaging, it is of course also possible to scan the patient subsequently with low and high tube voltage to generate dual energy data (Dual Spiral Dual Energy, available since 2011). Another option is to switch the tube voltage between two gantry rotations in a single scan (slow kV switching, implemented in some Toshiba scanners e.g. Toshiba Aquilion ONE) [13]. The history of DECT is summarized in Fig. 2.

For clinicians who are not familiar with dual energy imaging, the market might be confusing and misleading since different vendors use different marketing naming strategies for the same solution (see Tab. 1) – low and high energy data that are combined to a dual energy image. No matter how vendors may name their product, the currently available clinical CT products are and remain dual energy, i.e. data acquired at two different energies. Even more confusing is the fact that recently photon counting is emerging in the scientific community with prototype systems from Siemens Healthineers [14]–[17] or Philips [18] researching a new detector technology that enables true spectral (i.e. multi energy) imaging (see more in chapter "Outlook: Photon-counting detectors as a next step in multi-energy imaging").

Siemens Healthineers offers their dual energy imaging solutions as "Dual Energy" with different technological approaches (Dual Spiral Dual Energy, TwinBeam Dual Energy, and Dual Source Dual Energy). GE Healthcare uses "Gemstone Spectral Imaging" (GSI or GSI Xtream) as naming for their fast kV switching dual energy. Philips employs a dual layer detector in the IQon Spectral CT. Toshiba again promotes a different "Dual Energy" solution. Their approach can be best described as a slow kV switching where they take a full rotation at high energy followed by a full rotation at low energy to compose a dual energy data set.

With so many different naming strategies and solutions in the market it is the goal of this White Paper to look at the different options in more detail and to demonstrate the advantages and disadvantages within the following sections.

Table 1: Overview of the commercial dual energy solutions in the market:

Company	Marketing Name	Technology
Siemens Healthineers	Dual Energy	Dual Spiral
Siemens Healthineers	Dual Energy	TwinBeam
Siemens Healthineers	Dual Energy	Dual Source
GE Healthcare	Gemstone Spectral Imaging (GSI & GSI Xtream)	Fast kV switching
Philips Healthcare	Spectral CT (IQon Spectral CT)	Dual layer detector
Toshiba Medical Solutions	Dual Energy	Slow kV switching

3. DECT quality criteria

Image quality is crucial for reliable DECT imaging since dual energy data processing is sensitive to small changes of the Hounsfield units. Relevant criteria comprise the spectral separation and temporal coherence of the low and high energy data, as well as the temporal and spatial resolution of the CT images, but of course also the dose efficiency or the workflow aspects play an important role in enabling efficient DECT imaging in daily routine. Refs [19]–[21] discuss the different DECT approaches in some of these regards. All these aspects will be evaluated within the next chapters of this whitepaper.

Spectral separation

The spectral separation manifests itself in the overlap of the detected low and high energy X-ray spectrum, with a better spectral separation meaning less overlap. This is relevant for reliable and quantitative material decomposition, as illustrated in Fig. 3. The spectral separation can be evaluated quantitatively for example as the iodine ratio (ratio = HU @low energy/HU@high energy). A larger iodine ratio means a better spectral separation. This ratio describes how well a material can be separated from soft tissue or water-like materials that have a ratio of 1 (i.e. same CT value in low and high energy image, see Fig. 4). This is also directly related to radiation dose: Better spectral separation means less dose is required to obtain the same image quality [10], [21].

Fig. 3: Illustration of the impact of spectral separation on the differentiation of two materials (i.e. like the differentiation of bone marrow edema). The single energy gray-scale image (left) does not allow to differentiate the two materials present here. DECT with a bad and inferior spectral separation (middle; i.e. kV switching, dual layer detector, split filter) allows material differentiation but not well separated (noise in the green/orange material space). With excellent spectral separation the differentiation is clear (right; i.e. dual source technology).

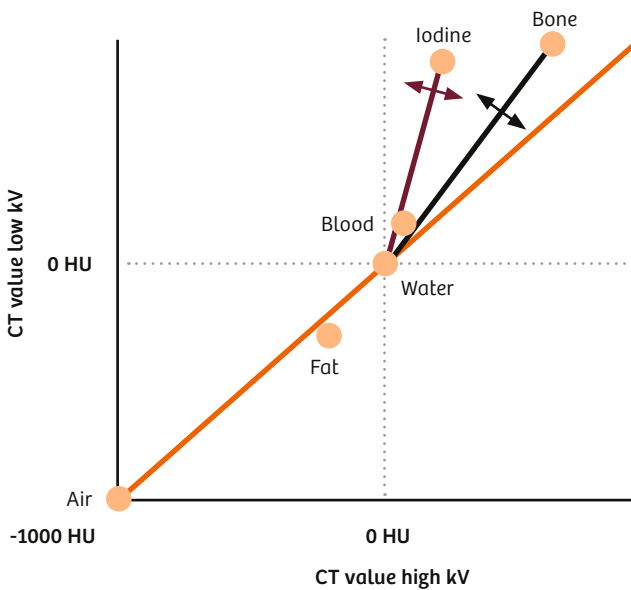## Bad spectral separation
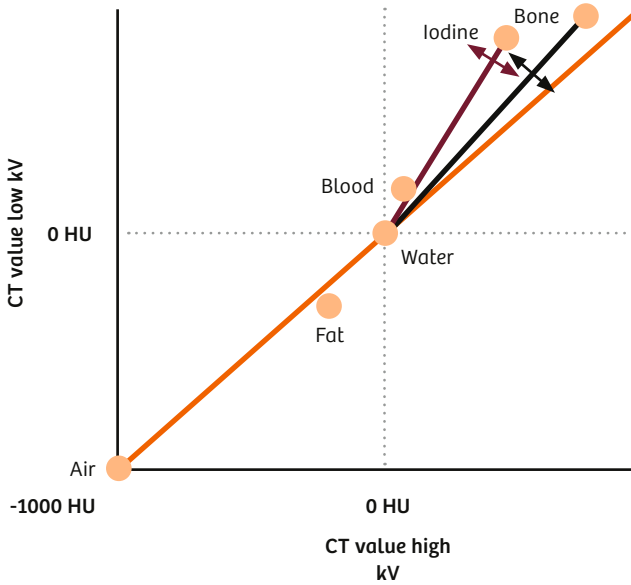
Good spectral separation

Fig. 4: Spectral separation as defined by the material characteristic slope (e.g. iodine ratio) in the dual energy diagram. The arrows orthogonal to the iodine (orange) and bone vector (gray), illustrate a certain noise level defined by the dose used for the image acquisition. At a higher dose this spread will become smaller. With a bad spectral separation (upper) this noise leads to misclassification of certain voxels, i.e. cross-talk between the two materials. This situation can be improved by using a higher dose. With a good spectral separation (lower) a higher noise level can be tolerated without significant cross-talk. This corresponds to the situation shown in the middle and on the right in Fig. 3.

Dual Spiral	The 80 kV/140 kV tube voltage combination provides a good spectral separation.
TwinBeam	The 120 kV spectrum used in TwinBeam mode is filtered by either tin (high energy) or gold (low energy) to generate two different spectra. The separation of these two spectra is moderate.
Dual Source	With its two independent tubes operated at two different voltages and the possibility to add a tin filter for the high energy spectrum, Dual Source Dual Energy can by far provide the best available spectral separation [10].
Fast kV switching	The fast switching of the tube voltage between nominally 80 kV and 140 kV cannot be performed in the desired rectangular manner, but the kV switching has significant transition times leading to a rather sinusoidal modulation curve. This results in blurred spectra and an inferior spectral separation below the one of Dual Spiral Dual Energy at true 80 kV/140 kV.
Dual layer detector	With this approach the energy separation is not achieved at the tube level as with all the other approaches, but on the detector level after the patient. A fixed kV together with a detector consisting of two stacked scintillator layers is used to extract low and high energy data. The idea is that the top scintillator layer absorbs the low energy part of the incident spectrum and the bottom layer the high energy part that has penetrated the top layer. The absorption process in the scintillator is of statistical nature, leading to a strong overlap in the detector low and high energy spectrum [22]. The fixed kV has to be either 140 kV or 120 kV; no DE post-processing is available for 100 kV or 80 kV. The spectral separation of the dual layer detector is a little better at 140 kV than at 120 kV, but using 140 kV has potential dose penalties. Also in this case the spectral separation is inferior to the one of Dual Spiral Dual Energy.
Slow kV switching	Due to the slower switching of the tube voltage compared to fast kV switching, the spectral blurring in the transition time is irrelevant, leading to a better spectral separation on the level of a Dual Spiral Dual Energy scan.

The spectral separation also has a direct impact on iodine quantification accuracy. Ref. [23] compared the iodine quantification accuracy of Dual Source and Dual layer detector DECT in a phantom study. A similar phantom was used in Ref. [24] to study the quantification accuracy with fast kV switching. Dual Source DECT at 70 kV/Sn150 kV showed a high accuracy in this comparison with a median measurement error of only -0.5% across different phantom sizes and iodine concentrations. At 80 kV/Sn150 kV the median error was -2.3%. Dual layer detector DECT exhibited a median measurement error of -4.6% at 120 kV and -3.3% at 140 kV. Fast kV switching underestimated the iodine concentration by up to -10% for the medium phantom size, -26% for the large phantom, and -33% for the obese phantom across different iodine concentrations. Dual Source DECT's median measurement error did not exceed a maximum absolute value of 5% for the different phantom sizes.

Ref. [25] and Ref. [26] report on distinguishing enhancing from non-enhancing renal lesions with DECT as an indicator for the separation of cysts from solid tumors. Ref. [25] employed a SOMATOM Definition Dual Source CT at 80 kV/140 kV still without the additional tin filter and used a threshold of a measured iodine concentration in the lesion of 0.5 mg/mL for the separation between enhancing and non-enhancing, yielding a sensitivity of 100%, a specificity of 97.7%, a positive predictive value of 97.2%, and a negative predictive value of 100% with histopathologic analysis or follow-up CT as the gold standard. The fast kV switching approach used in Ref. [26] required a much higher iodine concentration threshold of 2 mg/mL for the best separation, resulting in a sensitivity of 90%, a specificity of 93.7%, a positive predictive value of 81.8%, and a negative predictive value of 96.7%. The reference standard was in this case a change in lesion attenuation threshold of 20 HU between the unenhanced and the enhanced scan. This difference in the iodine concentration threshold and the resulting characterization accuracy may be related to the iodine quantification accuracy and thus the spectral separation.

Temporal coherence

Temporal coherence denotes the time delay between the acquisition of the low and high energy data. Ideally, this delay is as small as possible to avoid misregistration due to motion or problems with contrast agent dynamics e.g. a change in contrast agent concentration over time. A low temporal coherence may lead to increased misalignment between the low and high energy images, which in turn may lead to artefacts in the post-processed images (Fig. 5). It is important to note that a high temporal coherence alone does not help much without a good temporal resolution, which will be discussed in the next chapters.
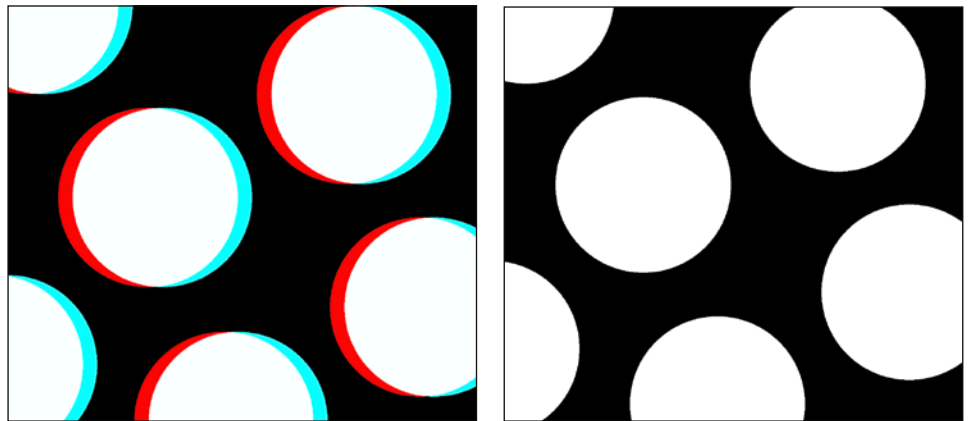
Fig. 5: A low temporal coherence (left) in combination with moving objects can lead to artefacts, a high temporal coherence helps to avoid such problems.

|	
Dual Spiral	This approach has a low temporal coherence. The delay is one scan time plus the time to move the table back. The absolute delay depends thus on the scan range and the scan speed. Nevertheless, this approach is therefore not recommended for CTA or imaging of moving structures like the thorax, but the focus should be on static structures (i.e. gout in extremities).
TwinBeam	The temporal coherence of this acquisition mode is high and can be as good as one rotation time, rendering it suitable for studies with contrast agent.
Dual Source	The dual energy data are acquired simultaneously with a 90° offset in projection space. Therefore the temporal coherence is very good, enabling even cardiac dual energy imaging.
Fast kV switching	The offset between the low and high energy projections is very short: It is the time to acquire one projection. Therefore, the temporal coherence in this case is also very good.
Dual layer detector	The dual layer detector has a perfect temporal coherence because the two scintillator layers are directly above each other.
Slow kV switching	The temporal coherence is at least one rotation time offset plus potential changeover times, which can be about 0.5 s [27].
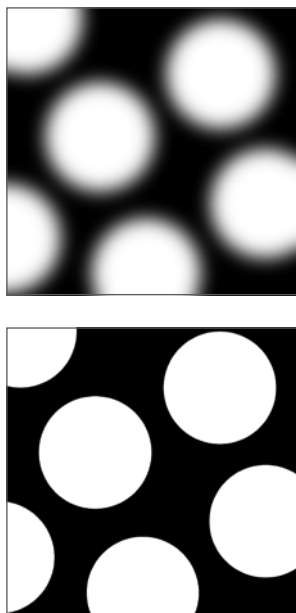
Fig. 6: With motion, a low temporal resolution (upper) leads to blurred images. High temporal resolution (lower) renders motion less problematic.
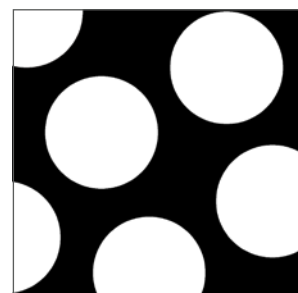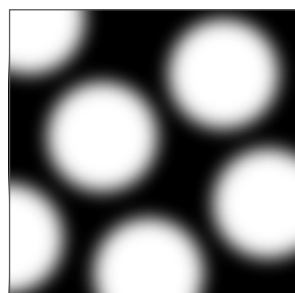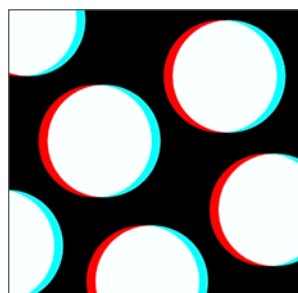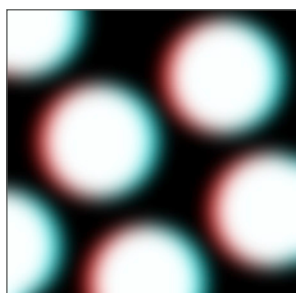
Temporal resolution

The temporal resolution of the low and high energy images is defined as the time required collecting the data for image reconstruction, which is usually half a rotation time. This is independent of the respective dual energy approach, except for Dual Source DECT where a special algorithm allows combining 90° of data from the two systems to reconstruct images with a temporal resolution of about a quarter rotation time. The temporal resolution determines the amplitude of motion artefacts, see Fig. 6. Temporal resolution should be clearly differentiated from temporal coherence, but they should be considered together. Think about sharp images (high temp. res.) with possible slight misregistration (sub-perfect temp. coherence; misregistration can be corrected by image registration) vs. blurred images (low temp. res.) that are perfectly registered (perfect temp. coherence). Obviously, the first scenario has benefits over the second one (Fig. 7).

Dual Spiral	Half a rotation time (0.28 s, 0.33 s, … depending on system)
TwinBeam	Half a rotation time (0.28 s–0.33 s depending on system)
Dual Source	Half a rotation time with rotation times down to 0.25 s, depending on system. Additional reconstruction available without DE information but with full Dual Source temporal resolution of about a quarter rotation time possible by combining the low and high energy data from two 90° segments.
Fast kV switching	Half a rotation time; however, most protocols use a rotation time of ≥ 0.5 s which therefore offers the lowest temporal resolution of all dual energy approaches
Dual layer detector	Half a rotation time; down to 0.27 s in cardiac mode [28]
Slow kV switching	Half a rotation time; rotation times down to 0.35 s have been reported [13]

Low temporal coherence   **High temporal coherence**

1

2

3

4

Fig. 7: Illustration of the combination of temporal resolution and temporal coherence in the context of moving objects. For stationary objects this is not relevant. A low temporal resolution in combination with a low temporal coherence will generate blurred and offset images (1), i.e. Dual Spiral Dual Energy at slow rotation times (1 s) and low pitch values (~0.5). A high temporal resolution with a low temporal coherence (2); i.e. Dual Spiral Dual Energy at fast rotation times (0.3 s) and high pitch (~1) leads to sharp but slightly offset images. If the temporal resolution is low but the coherence high, the images are blurred but well registered (3); i.e. fast kV switching at pitch ~1 and 0.6 s rotation time. A high temporal resolution in combination with a high coherence leads to best results (4; i.e. Dual Source Dual Energy at pitch ~1 and 0.25 s rotation time).

Spatial resolution

Spatial resolution is an important image quality parameter regarding the visualization of small objects, i.e. image "sharpness", as illustrated in Fig. 8. Assuming that the image data is not already blurred from bad spectral separation, motion and a bad temporal resolution, the spatial resolution is mainly determined by focal spot size, detector element size, and the number of projections per rotation. As a side note it should also be mentioned that the detectability of small structures like iodine in small vessels or the characterization of small kidney stones is not only related to the spatial resolution but also to the spectral separation.

Dual Spiral	Full system capabilities available, i.e. full number of projections for low and high energy data and regular focal spot size
TwinBeam	Full system capabilities available, i.e. full number of projections for low and high energy data and regular focal spot size
Dual Source	Full system capabilities available, i.e. full number of projections for low and high energy data and regular focal spot size
Fast kV switching	Degraded spatial resolution due to an extra-large focal spot (2.0 x 1.2 IEC 60336:2005) and a limited number of projections per energy. The available approach uses a low energy : high energy sampling of 2 : 1 since more dose at 80 kV is required. At a total number of 1968 projections per rotation, this leads to 1312 low energy projections and only 656 high energy projections. Especially the latter is a low number compared to other techniques. All this will result in a blurring of the images due to a significant loss of spatial resolution compared to a normal non dual energy scan.
Dual layer detector	Full system capabilities available, i.e. full number of projections for low and high energy data and regular focal spot size
Slow kV switching	Full system capabilities available, i.e. full number of projections for low and high energy data and regular focal spot size

Fig. 8: Low spatial resolution (left) caused e.g. by a large focal spot or by a low number of projections renders a clear visualization of objects difficult, especially for small objects. A high spatial resolution (right) generates a sharp delineation of objects.

Dose efficiency

DECT can provide additional diagnostic information. However, this should not come at the expense of an increased patient dose compared to a conventional single energy examination. Therefore, it is important that the respective DECT solutions are supporting all state-of-the-art dose reduction features like tube current modulation or iterative reconstruction to allow dose neutral DECT scanning. It is important to note that also the spectral separation plays an important role here since a system with better spectral separation allows achieving a certain material image quality with less dose than a system with worse spectral separation [10], [21].

Dual Spiral	CARE Dose4D tube current modulation for best adaptation to patient habitus; tube current for low and high energy scans set independently for optimal results; iterative reconstruction applicable
TwinBeam	CARE Dose4D tube current modulation for best adaptation to patient; TwinBeam filter removes low energy photons for higher dose efficiency; iterative reconstruction applicable
Dual Source	CARE Dose4D tube current modulation for best adaptation to patient for both tubes; tube current can be set independently for optimal results; iterative reconstruction applicable
Fast kV switching	Limitations in today's X-ray tube technology do not allow for a fast modulation of the tube current [29]. This has two drawbacks in the case of fast kV switching: tube current modulation is not possible and the tube current cannot be set to different levels for the low and the high tube voltage, which would be required to achieve the desired similar noise level in the low and high energy data. Additionally, the tube current has to be fixed at a relatively high level to allow stable switching of the tube voltage. All this leads in many cases to a higher exposure to that of standard single energy scans with tube current modulation [8], [30]–[31], which may only partially be compensated by iterative reconstruction.

Dual layer detector	Tube current modulation and iterative reconstruction are available. In case of a dual layer detector it is important to note that the noise level in the low and high energy data is determined by the thickness of the two stacked detector layers, which can only be optimized for a certain tube voltage and patient diameter. Small patients like babies and very large patients will therefore yield suboptimal results.
Slow kV switching	Tube current modulation is available and due to the slower switching between rotations instead of projections it is possible to set the tube current to two different levels for the low and high tube voltage. Iterative reconstruction is available. Another advantage is the possibility to protect dose sensitive organs by turning off or at least reducing the radiation over a certain range.

Summary:

Dual Energy is meanwhile available with different solutions and also applicable in clinical routine. Nevertheless the different approaches come along with advantages and drawbacks in specific categories which are of relevance for image quality.

Dual Spiral offers an entry level solution which has some drawbacks in regards to temporal coherence and the usage of applications which involve contrast media agent. Nevertheless it can be used for advanced diagnostic performance in clinical routine in specific clinical fields.

Looking at the number of published scientific articles, slow kV switching shows a very limited impact in clinical routine and also faces some drawbacks which other solutions can overcome in most of the categories.

Without the ability to apply a dose modulated scan, the low temporal resolution (slower rotation time), a degraded spatial resolution (large focal spot, low number of projections) and an inferior spectral separation, fast kV switching also can be seen as an inferior solution compared to other technologies.

The TwinBeam and dual layer detector approach can be seen as similar concerning spectral separation. While the first splits the X-ray beam before the patient, dual layer detector technology splits the X-ray beam after the patient. Both approaches show advantages over the above mentioned technologies but nevertheless are also having draw backs compared to Dual Source Dual Energy.

Besides the smaller FoV, Dual Source Dual Energy is in all categories either equal or superior to the compared approaches and can therefore be seen as a solution in its own league. Especially the excellent spectral separation with a dedicated tin filter, the full spatial and temporal resolution, the excellent temporal coherence, the high dose efficiency and the specific energy pairings for specific protocols deliver a clinical solution that is unmatched in the market and was one of the core reasons for Siemens to invest in the innovation of Dual Source technology.

4. Dual Energy Postprocessing

DECT imaging acquires more data than conventional single energy scans. While it is a diagnostic advantage to have the possibility to gain additional information from DECT imaging, image acquisition and postprocessing should not interfere with the clinical workflows and data management should not become an issue. This requires software features allowing automatic data handling and a ready-to-read presentation of the resulting images. Within the postprocessing section this white paper will focus on Siemens Healthineers' solution.

In the past, dual energy postprocessing needed an extra interplay of the user with a *syngo*.via workstation. Nevertheless clinicians want their images PACS-ready and not need to invest time in additional postprocessing steps. Therefore Siemens Healthineers has created different solutions to deliver PACS-ready images with dual energy scanning from basic to advanced postprocessing.

Basic postprocessing with FAST DE and FAST DE Results:

FAST DE (for Dual Source systems only) directly reconstructs mixed images with an adjustable weighting factor for different use-cases at the scanner which can be sent directly to PACS.

FAST DE Results allows choosing different types of post-processing directly at the scanner and sending the resulting images to PACS. Retrospective modification of algorithm parameters can be undertaken in *syngo*.via if necessary.

Advanced postprocessing with *syngo*.via Rapid Results Technology for Dual Energy:

Rapid Results improves your efficiency by reducing several workflow steps. It enables direct communication between *syngo*.via and SOMATOM CT scanners, triggering zero-click post-processing within the selected scan protocol. In that way, *syngo*.via automatically creates and sends ready-to-read results wherever you are, to your PACS or a film printer.
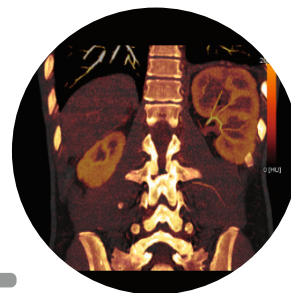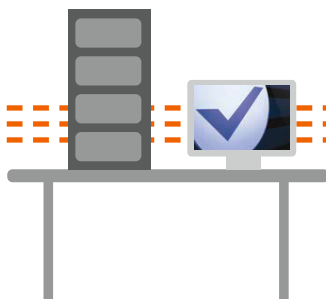
SOMATOM CT scanner

Rapid Results Technology helps you make dual energy routine, with no need to change your clinical workflow. Rapid Results will automatically generate standard visualizations of different anatomies in the required orientation and thickness. Just define your workflow once and let Rapid Results produce the decision basis, from virtual unenhanced images or iodine maps – key in oncology cases – to monoenergetic images for metal artifact reduction or contrast improvements, and Lung PBV maps for pulmonary embolism assessment. Equipped with the Rapid Results technology, you are prepared for an emergency – e.g., at night, when experienced operators may not be available.

. . . .

Your benefits with Rapid Results Technology:

1   **Clinical innovations like Monoenergetic Plus imaging for routine exams regardless of expertise level**

2   **Standardized and consistent image quality independent of operator**

3   **Post-processing becomes part of the standard reconstruction task**

4   **Ready-to-read results wherever you want them**

. . . .

syngo.via server   **PACS**

5. Clinical applications

More and more radiologists are relying on the rich diagnostic possibilities offered by Dual Energy imaging on our CT scanner fleet ranging from our SOMATOM® go.Top[1] up to our outstanding SOMATOM® Force. The question is: What makes Dual Energy stand out in your daily practice? Look for these three criteria:

- Crisp images with the option for even sharper contrast and significant metal artifact reduction
- No extra dose [32]–[35] compared to conventional imaging at 120 kV and
- Broad applicability for virtually all your clinical questions and patients.

Simplifying Routine

Perform zero-click post-processing with Rapid Results and integrate Dual Energy techniques and applications into your daily clinical routine. Your reconstructed images are automatically post-processed and then sent to your PACS without the need for manual interaction of your staff or yourself.

Empowering Innovation

Gain clinical information beyond morphology and highlight, characterize, quantify, and differentiate the material in your scans with DECT. Challenge your status quo and proactively push your medical progress further.

Adapting to you

All your patients are different and your need for further diagnostic capabilities and information varies in every case? Dual Energy offers you dedicated protocols and evaluation software applications for virtually all types of patients and a wide range of your clinical questions.

Standard Functionality

Every *syngo*.via already includes standard CT applications that provide an extensive range of functions and tools required for a variety of specific clinical fields, such as CT Dual Energy reading, among others. *syngo*.via includes what is needed to read and share CT images and results.

syngo.CT Dual Energy

Optimum Contrast for sharper image contrast

Optimum Contrast is an intelligent method that changes the blending ratio of low- and high-energy data on a pixel-by-pixel basis, depending on the corresponding Hounsfield units (CT numbers). For higher CT numbers, which occur in regions of high iodine concentration, larger proportions of the image are taken from low tube-energy data. As a result, areas of contrast enhancement are accentuated.

Monoenergetic imaging for reducing metal artifacts or improving iodine contrast

With monoenergetic imaging, metal artifacts can be reduced in both Single Source and Dual Source Dual Energy data. Select the energy level at which implants, clamps, or screws will have the smallest impact on image quality and get unsurpassed scan results.

[1] This product is pending 510(k) clearance, and is not yet commercially available in the United States

Chemical characterization of different materials

The attenuation of X-rays, among others, depends on the electron density and the effective atomic number. Both parameters are characteristic for different materials. With *syngo*.CT DE Rho/Z, you have access to electron density and effective Z maps in one examination.

Advanced Package
## Accurate and non-invasive diagnosis of gout *syngo*.CT DE Gout

syngo.CT DE Gout facilitates the visualization of deposited uric acid crystals in peripheral extremities by automatically color-coding these crystals to visualize those deposits. Conventional methods of diagnosing gout, for example the aspiration of the joint, are limited in feasibility – especially in acute cases where the joint is inflamed and painful. In these cases an aspiration may not be performable and gout can be difficult to diagnose because there are various forms of arthritis that have similar symptoms.

syngo.CT DE Gout overcomes these limitations by being non-invasive, more specific, and fast. It also provides insight into areas that cannot be reached by conventional aspiration, since uric acid crystals can also be located in periarticular soft tissues, such as tendons and ligaments. [36]

Characterization of kidney stones
## *syngo*.CT DE Calculi Characterization

syngo.CT DE Calculi Characterization allows identification and characterization of different kinds of kidney stones. [37] The basis for this approach is the utilization of DE CT data in order to calculate a visual color-coded material decomposition into uric acid and other stone types. *syngo*.CT DE Calculi Characterization also includes the Kidney Stone Navigator for handy review and evaluation of all potential stones that have been identified.
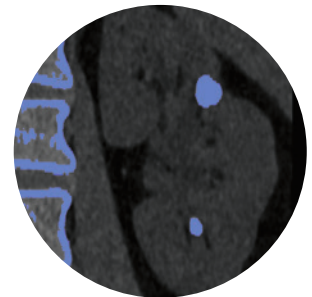
Quantify lesions with two scans in one
syngo.CT DE Virtual Unenhanced

In modern oncology, CT imaging plays a major role in treatment decisions and follow-ups of current therapy. Especially important are the localization and the characterization of lesions in order to rule out malignancy. With DE, it is possible to perform a contrast scan and to view a virtual non-contrast image retrospectively. [38] Another advantage of DE CT is the ability to quantify the iodine uptake [mg/mL] in tissue and lesions.

The iodine uptake may correlate with the malignancy of a lesion. This capability also may help in follow-up scenarios where the effectivity of a therapy can be validated by evaluating the development of the iodine uptake of the treated lesion. *syngo*.CT DE Virtual Unenhanced has been extended by optimized visualization of other organs apart from the liver. Virtual non-contrast (VNC) imaging has been successfully applied for kidney, pancreas, lung, aorta and lymph nodes. For the evaluation of liver lesions, *syngo*.CT DE Virtual Unenhanced still includes the well established application Liver VNC with an algorithm optimized for liver tissue.
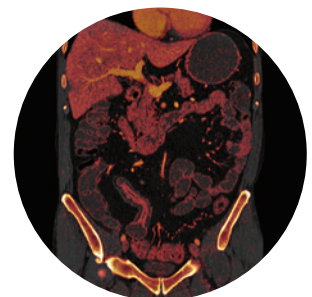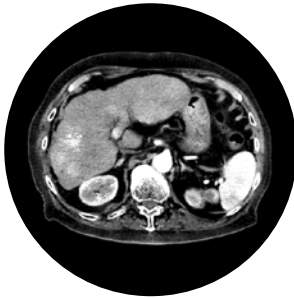
Maximize image quality with new algorithm
syngo.CT DE Monoenergetic Plus

Monoenergetic imaging has become a reliable routine tool for image quality enhancement [39] and metal artifact reduction. The DE application *syngo*.CT DE Monoenergetic Plus allows users to display monoenergetic images in a range of 40–190 keV. By displaying multiple monoenergetic regions of interest and the associated absorption curves, Monoenergetic Plus lets users easily compare and quantify lesions and tissues.

The ability to export statistical information for further evaluation is very beneficial for various research and diagnostic tasks. In addition, high enhancement is observed even for low iodine concentrations at low energy levels.
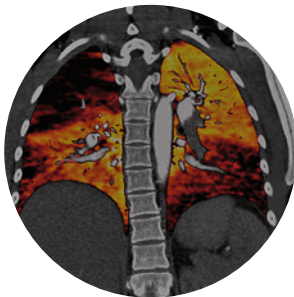
Assessment of perfusion defects and affected vessels at a glance
syngo.CT DE Lung Analysis

syngo.CT DE Lung Analysis is a combination of *syngo* Dual Energy Lung Vessels and *syngo* Dual Energy Lung PBV. *syngo*.CT DE Lung Analysis allows the color-coding of vessels that are affected, e.g., by pulmonary emboli and therefore show a significantly lower iodine concentration than nonaffected vessels. It also enables fast evaluation of the related lung perfusion defects without the use of an additional non-contrast scan. *syngo*.CT DE Lung Analysis directly visualizes the local iodine concentration in the lung parenchyma, which is a measure of the local blood volume, thus enabling a display of the area of possibly affected tissue. The application provides you with the needed diagnostic information at a glance. [40]


Accurate bone removal even in complex body regions
syngo.CT DE Direct Angio

syngo.CT DE Direct Angio accurately highlights vessel structures on CT angiography (CTA) data sets, and suppresses bone structures to provide you with a bone free view of the vessel system, e.g., to subtract bone in CTAs. Overcoming limitations of conventional bone removal software, the DE approach reliably isolates even complex vasculature, such as at the base of the skull, where CTAs are difficult to interpret. [41]

Differentiate calcified plaques from iodine contrast
*syngo*.CT DE Hardplaque Display

In contrast-enhanced CT scans of the vessel system (CTA), it can be difficult to differentiate between calcified plaques and iodine contrast. Also the plaque can make it quite challenging to assess the grade of the stenosis. *syngo*.CT DE Harplaque Display enables the identification (color-coding) and automatic removal of calcifications from a DE CTA image. This helps differentiating hard plaques from contrast agent. [42]
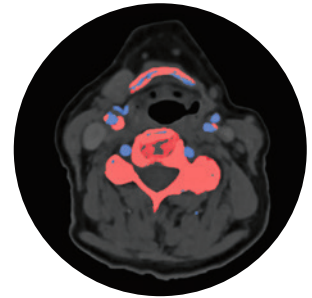
## Evaluation of the bone marrow
syngo.CT DE Bone Marrow

Bone marrow can be affected by various pathologies, such as bone bruises after trauma and diffuse tumor infiltrations. Up to now, the major modality for imaging these pathologies has been MRI. With the benefits of Dual Energy, CT imaging can now also aid in the diagnosis. [43]

The DE application *syngo*.CT DE Bone Marrow allows for the segmentation and visualization (color-coding) of the bone marrow based on a material decomposition into bone marrow and calcium. This application can be used both for Dual Source and Single Source data sets.
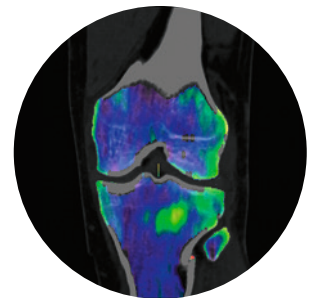

Differentiate hemorrhage from iodine-uptaking bleeds and lesions
syngo.CT DE Brain Hemorrhage

The DE application *syngo*.CT DE Brain Hemorrhage assists you in visualizing iodine concentration and distribution in the brain. Lesions and bleeds may show significant iodine uptake in the image, while inactive hemorrhages are not enhanced. [44]
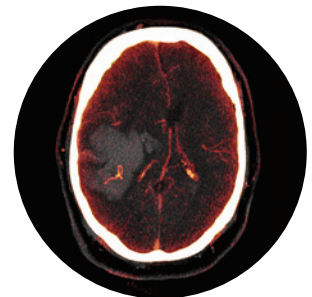
Reveal perfusion defects with only one scan
syngo.CT DE Heart PBV

This application uses DE information to visualize and quantify the iodine concentration in the myocardium to reveal perfusional defects. [45] In addition, a virtual noncontrast display can be used to identify myocardial edema. Simultaneous acquisition of the high- and the low-kV datasets diminishes the problem of misregistration due to cardiac motion.
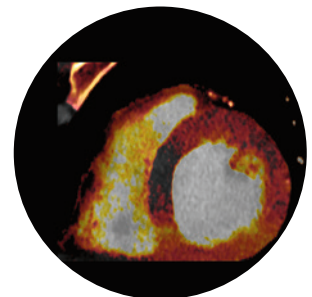
6. Outlook: Photon-counting detectors as a next step in multi-energy imaging

Within the last years a new technology has shown up in the clinical research environment with some prototype installations: photon counting detectors. Besides other benefits one of the core benefits will be a full multi-energy acquisition in every scan.

Today's solid-state detectors use a two-step process to convert the incoming X-ray intensity into an electronic signal. First, the X-rays are converted into visible light in a scintillator layer. Below, the figure shows a photodiode array that converts the emitted light into an electric current that is digitized in dedicated ASICs. The scintillator layer is made of a ceramic material that is mechanically structured into pixels. Septa of finite width separate the individual pixels in order to suppress optical cross-talk (Fig. 9). While today's dual energy technology with this detectors is based on different technical approaches and either generated by splitting the X-ray beam or using existing detector technology with different layers, the limitation remains the same: A set of only two more or less clearly separated dual energy images is generated in any case.

The next step: photon-counting detectors

Recent research approaches for a next generation detector technology shows promising results. Semiconductor materials such as cadmium telluride (CdTe) are able to convert X-rays directly into electric signal pulses. Each incoming X-ray quantum generates clouds of free charge carriers with the amount of free charges being proportional to the energy of the incident X-ray photon. A strong electrical field inside the detector material transports the charge clouds to anode pixels (Fig. 10) in which an electrical current is induced. Highly integrated circuits transform these charge pulses into voltage pulses of a few nanoseconds duration that can be counted digitally.

Multi-energy information

If such detectors will become available, they will offer tremendous advantages. It would not only be possible to register or count each individual photon but also to measure the energy from each individual photon. Without any other technical prerequisites, multi-energy CT (real spectral imaging) could become possible. In principle, as a next step following on from dual energy CT, an arbitrary number of energies is achievable. Still, in order to limit the amount of data delivered by the detector, it is more practical to put the registered photons within certain energy ranges or "energy bins" and only read the data for these bins. Today's dual energy CT is sufficient for the materials present in the human body and for iodine contrast. More "bins" would not really add more information here. Should new contrast materials become available in the future, however, such as gold nanoparticles with additional absorption peaks in the used X-ray energy range, [46] three, four, or even more, bins might be beneficial (K-edge imaging).
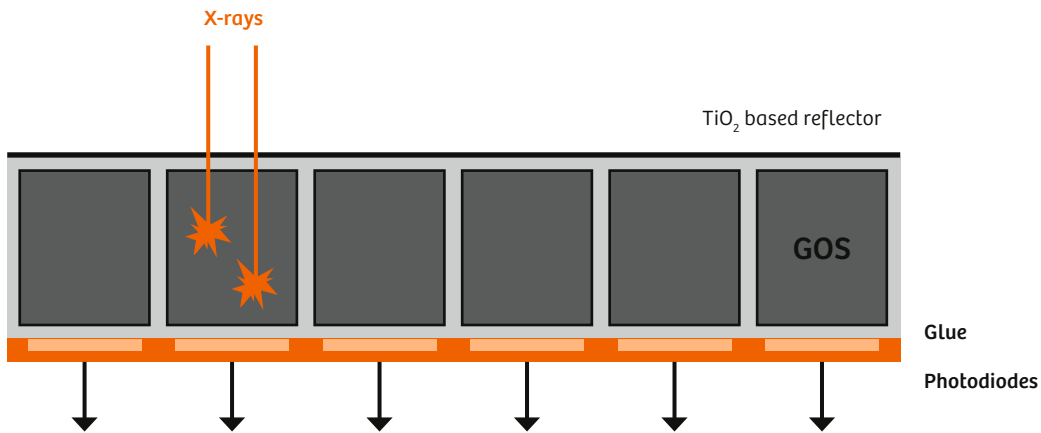
Fig. 9: Energy-integrating detectors convert X-rays into an electrical signal in a two-step process: First, a scintillator layer (GOS) converts X-rays into visible light. Photodiodes then convert light into an electrical current.
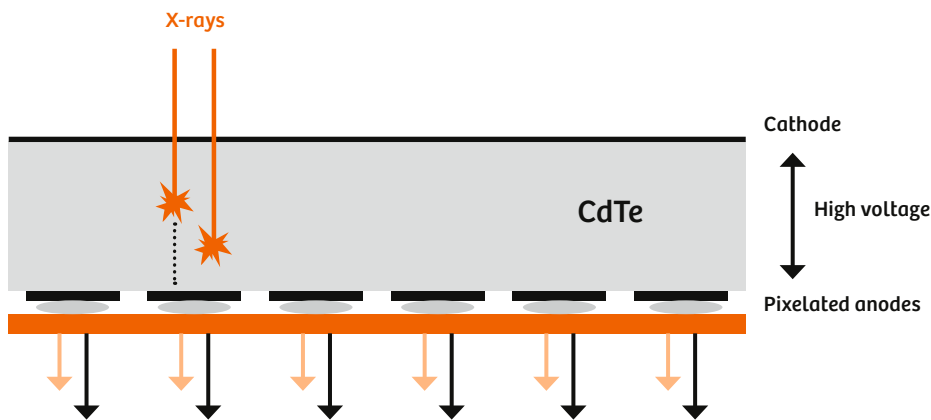

Fig. 10: Certain materials (e.g., CdTe) can directly convert X-rays into an electrical current. Each photon can be detected individually and its energy can be measured.

Prototype installations

Siemens Healthineers is the first medical equipment company to be able to demonstrate the potential of high-flux capable photon-counting technology in two near-clinical prototype installations. [47]–[49] The prototypes are based on SOMATOM Definition Flash hardware in which the second detector system was replaced with a photon-counting detector. For the first time, clinical equivalence comparable to existing technology was demonstrated in human subjects. In the next years, Siemens Healthineers will collaborate with its network of partners to optimize the technology and to identify new clinical potentials.

7. References

[1] R. E. Alvarez and A. Macovski, "Energy-selective reconstructions in x-ray computerised tomography," Phys. Med. Biol., vol. 21, no. 5, p. 733, 1976.

[2] R. A. Brooks, "A Quantitative Theory of the Hounsfield Unit and Its Application to Dual Energy Scanning.," J. Comput. Assist. Tomogr., vol. 1, no. 4, 1977.

[3] W. A. Kalender, W. Perman, J. Vetter, and E. Klotz, "Evaluation of a prototype dual-energy computed tomographic apparatus. I. Phantom studies," Med. Phys., vol. 13, no. 3, pp. 334–339, 1986.

[4] T. G. Flohr et al., "First performance evaluation of a dual-source CT (DSCT) system," Eur. Radiol., vol. 16, no. 2, pp. 256–268, 2006.

[5] A. Primak, J. Ramirez Giraldo, X. Liu, L. Yu, and C. H. McCollough, "Improved dual-energy material discrimination for dual-source CT by means of additional spectral filtration," Med. Phys., vol. 36, no. 4, pp. 1359–1369, 2009.

[6] D. Zhang, X. Li, and B. Liu, "Objective characterization of GE discovery CT750 HD scanner: gemstone spectral imaging mode," Med. Phys., vol. 38, no. 3, pp. 1178–1188, 2011.

[7] R. Zhang, J.-B. Thibault, C. A. Bouman, K. D. Sauer, and J. Hsieh, "Model-based iterative reconstruction for dual-energy X-ray CT using a joint quadratic likelihood model," IEEE Trans. Med. Imaging, vol. 33, no. 1, pp. 117–134, 2014.

[8] B. Li, G. Yadava, and J. Hsieh, "Quantification of head and body CTDIVOL of dual-energy x-ray CT with fast-kVp switching," Med. Phys., vol. 38, no. 5, pp. 2595–2601, 2011.

[9] M. Gabbai, I. Leichter, S. Mahgerefteh, and J. Sosna, "Spectral material characterization with dual-energy CT: comparison of commercial and investigative technologies in phantoms," Acta Radiol., vol. 56, no. 8, pp. 960–969, 2015.

[10] B. Krauss, K. L. Grant, B. T. Schmidt, and T. G. Flohr, "The importance of spectral separation: an assessment of dual-energy spectral separation for quantitative ability and dose efficiency," Invest. Radiol., vol. 50, no. 2, pp. 114–118, 2015.

[11] A. Euler et al., "Initial Results of a Single-Source Dual-Energy Computed Tomography Technique Using a Split-Filter: Assessment of Image Quality, Radiation Dose, and Accuracy of Dual-Energy Applications in an In Vitro and In Vivo Study," Invest. Radiol., vol. 51, no. 8, pp. 491–498, 2016.

[12] B. Rutt and A. Fenster, "Split-filter computed tomography: a simple technique for dual energy scanning.," 1980.

[13] X.-R. Cai et al., "Iodine distribution map in dual-energy computed tomography pulmonary artery imaging with rapid kVp switching for the diagnostic analysis and quantitative evaluation of acute pulmonary embolism," Acad. Radiol., vol. 22, no. 6, pp. 743–751, 2015.

[14] Pourmorteza A, Symons R, Sandfort V, Mallek M, Fuld MK, Henderson G, et al. "Abdominal Imaging with Contrast-enhanced Photon-counting CT: First Human Experience." Radiology, vol. 279, no 1, pp. 239–245, 2016.

[15] Yu Z, Leng S, Jorgensen SM, Li Z, Gutjahr R, Chen B, et al. "Evaluation of conventional imaging performance in a research whole-body CT system with a photon-counting detector array." Physics in Medicine and Biology, vol. 61, no. 4, pp. 1572-1595, 2016.

[16] Symons R, Cork TE, Lakshmanan MN, Evers R, Davies-Venn C, Rice KA, et al. "Dual-contrast agent photon-counting computed tomography of the heart: initial experience." The International Journal of Cardiovascular Imaging, Vol. 33, no. 8, pp. 1253-1261, 2017.

[17] Symons R, Krauss B, Sahbaee P, Cork TE, Lakshmanan MN, Bluemke DA, et al. "Photon-counting CT for simultaneous imaging of multiple contrast agents in the abdomen: An in vivo study." Medical Physics, vol. 44, no. 10, pp. 5120.5127, 2017.

[18] Muenzel D, Bar-Ness D, Roessl E, Blevis I, Bartels M, Fingerle AA, et al. "Spectral Photon-counting CT: Initial Experience with Dual–Contrast Agent K-Edge Colonography." Radiology, vol. 283, no. 3, pp. 723-728, 2017.

[19] C. H. McCollough, S. Leng, L. Yu, and J. G. Fletcher, "Dual-and multi-energy CT: principles, technical approaches, and clinical applications," Radiology, vol. 276, no. 3, pp. 637–653, 2015.

[20] H. W. Goo and J. M. Goo, "Dual-Energy CT: New Horizon in Medical Imaging," Korean J. Radiol., vol. 18, no. 4, pp. 555–569, 2017.

[21] S. Faby et al., "Performance of today's dual energy CT and future multi energy CT in virtual non-contrast imaging and in iodine quantification: A simulation study," Med. Phys., vol. 42, no. 7, pp. 4349–4366, 2015.

[22] J. E. Tkaczyk et al., "Atomic number resolution for three spectral CT imaging systems," presented at the Medical Imaging, pp. 651009–651009 2007.

[23] G. J. Pelgrim, R. van Hamservelt, and M. J. Willemink, "Accuracy of iodine quantification using dual energy CT in latest generation dual source and dual layer CT," Eur Radiol Doi, vol. 10, 2017.

[24] A. E. Papadakis and J. Damilakis, "Fast kVp-switching dual energy contrast-enhanced thorax and cardiac CT: A phantom study on the accuracy of iodine concentration and effective atomic number measurement," Med. Phys., DOI: 10.1002/mp.12437

[25] A. Mileto et al., "Accuracy of contrast-enhanced dual-energy MDCT for the assessment of iodine uptake in renal lesions," Am. J. Roentgenol., vol. 202, no. 5, pp. W466–W474, 2014.

[26] R. K. Kaza, E. M. Caoili, R. H. Cohan, and J. F. Platt, "Distinguishing enhancing from nonenhancing renal lesions with fast kilovoltage-switching dual-energy CT," Am. J. Roentgenol., vol. 197, no. 6, pp. 1375–1381, 2011.

[27] T. Diekhoff et al., "Detection and characterization of crystal suspensions using single-source dual-energy computed tomography: a phantom model of crystal arthropathies," Invest. Radiol., vol. 50, no. 4, pp. 255–260, 2015.

[28] T. Hickethier et al., "Monoenergetic reconstructions for imaging of coronary artery stents using spectral detector CT: In-vitro experience and comparison to conventional images," J. Cardiovasc. Comput. Tomogr., 2017.

[29] G. M. Lu, Y. Zhao, L. J. Zhang, and U. J. Schoepf, "Dual-energy CT of the lung," Am. J. Roentgenol., vol. 199, no. 5_supplement, pp. S40–S53, 2012.

[30] S. Winklhofer, J. W. Lambert, Y. Sun, Z. J. Wang, D. S. Sun, and B. M. Yeh, "Pelvic Beam-Hardening Artifacts in Dual-Energy CT Image Reconstructions: Occurrence and Impact on Image Quality," Am. J. Roentgenol., vol. 208, no. 1, pp. 114–123, 2017.

[31] L. L. Geyer et al., "Imaging of acute pulmonary embolism using a dual energy CT system with rapid kVp switching: initial results," Eur. J. Radiol., vol. 81, no. 12, pp. 3711–3718, 2012.

[32] Purysko AS, Primak AN, Baker ME, Obuchowski NA, Remer EM, John B, et al. "Comparison of radiation dose and image quality from single-energy and dual-energy CT examinations in the same patients screened for hepatocellular carcinoma." Clinical Radiology [Internet], vol. 69, no. 12, pp. 538-544, 2014.

[33] Uhrig M, Simons D, Kachelrieß M, Pisana F, Kuchenbecker S, Schlemmer H-P. "Advanced abdominal imaging with dual energy CT is feasible without increasing radiation dose." Cancer Imaging [Internet], vol. 16, no. 1, 2016.

[34] Schenzle JC, Sommer WH, Neumaier K, Michalski G, Lechel U, Nikolaou K, et al. "Dual energy CT of the chest: how about the dose?" Invest Radiol, vol. 45, no. 6, pp347-353, 2010.

[35] Euler A, Parakh A, Falkowski AL, Manneck S, Dashti D, Krauss B, et al. "Initial Results of a Single-Source Dual-Energy Computed Tomography Technique Using a Split-Filter." Investigative Radiology [Internet], vol. 51, no. 8, pp. 491-498, 2016.

[36] Tashakkor AY, Wang JT, Tso D, Choi HK, Nicolaou S. "Dual-energy computed tomography: a valid tool in assessment of gout?" Int J Clin Rheumatol, vol. 7, no. 1, pp. 73-79, 2012.

[37] Graser A, Johnson TRC, Bader M, Staehler M, Haseke N, Nikolaou K, et al. "Dual Energy CT Characterization of Urinary Calculi: Initial In Vitro and Clinical Experience." Investigative Radiology, vol. 43, no. 2, pp. 112-119, 2008.

[38] Slebocki K, Kraus B, Chang D-H, Hellmich M, Maintz D, Bangard C. "Incidental Findings in Abdominal Dual-Energy Computed Tomography." Journal of Computer Assisted Tomography, vol. 41, no. 2, pp. 294-297, 2017.

[39] Albrecht MH, Scholtz J-E, Kraft J, Bauer RW, Kaup M, Dewes P, et al. "Assessment of an Advanced Monoenergetic Reconstruction Technique in Dual-Energy Computed Tomography of Head and Neck Cancer." European Radiology, vol. 25, no. 8, pp. 2493-2501, 2015.

[40] Takagi H, Ota H, Sugimura K, Otani K, Tominaga J, Aoki T, et al. "Dual-energy CT to estimate clinical severity of chronic thromboembolic pulmonary hypertension: Comparison with invasive right heart catheterization." European Journal of Radiology, vol. 85, no. 9, pp. 1574-1580, 2016.

[41] Naruto N, Tannai H, Nishikawa K, Yamagishi K, Hashimoto M, Kawabe H, et al. "Dual-energy bone removal computed tomography (BRCT): preliminary report of efficacy of acute intracranial hemorrhage detection." Emergency Radiology, vol. 25, no. 1, pp. 29-33, 2017.

[42] Uotani K, Watanabe Y, Higashi M, Nakazawa T, Kono AK, Hori Y, et al. "Dual-energy CT head bone and hard plaque removal for quantification of calcified carotid stenosis: utility and comparison with digital subtraction angiography." European Radiology, vol. 19, no. 8, pp. 2060-2065, 2009.

[43] Kellock TT, Nicolaou S, Kim SSY, Al-Busaidi S, Louis LJ, O'Connell TW, et al. "Detection of Bone Marrow Edema in Nondisplaced Hip Fractures: Utility of a Virtual Noncalcium Dual-Energy CT Application." Radiology, vol. 284, no. 3, pp. 798-805, 2017.

[44] Bodanapally UK, Dreizin D, Issa G, Archer-Arroyo KL, Sudini K, Fleiter TR. "Dual-Energy CT in Enhancing Subdural Effusions that Masquerade as Subdural Hematomas: Diagnosis with Virtual High-Monochromatic (190-keV) Images." American Journal of Neuroradiology, vol. 38, no. 10, pp. 1946-1952, 2017.

[45] Chung HW, Ko SM, Hwang HK, So Y, Yi JG, Lee EJ. "Diagnostic Performance of Coronary CT Angiography, Stress Dual-Energy CT Perfusion, and Stress Perfusion Single-Photon Emission Computed Tomography for Coronary Artery Disease: Comparison with Combined Invasive Coronary Angiography and Stress Perfusion Cardiac MRI." Korean Journal of Radiology, vol. 18, no. 3, pp. 476, 2017.

[46] Cormode DP, Naha PC, Fayad ZA. Nanoparticle contrast agents for computed tomography: a focus on micelles. Contrast Media Mol Imaging. Jan-Feb;9(1):37-52 2014.

[47] S. Kappler et al., First results from a hybrid prototype CT scanner for exploring benefits of quantum-counting in clinical CT, Proc. SPIE 8313, pp. 83130X 2012.

[48] Zhicong Yu, Shuai Leng, Steven M Jorgensen, Zhoubo Li, Ralf Gutjahr, Baiyu Chen, Ahmed F Halaweish, Steffen Kappler, Lifeng Yu, Erik L Ritman and Cynthia H McCollough. Evaluation of conventional imaging performance in a research whole-body CT system with a photon-counting detector array. Phys. Med. Biol. 61 1572–1595 2016.

[49] Pourmorteza A, Symons R, Sandfort V, Mallek M, Fuld MK, Henderson G, Jones EC, Malayeri AA, Folio LR, Bluemke DA. Abdominal Imaging with Contrastenhanced Photon-counting CT: First Human Experience. Radiology. Feb 3:152601 2016.

On account of certain regional limitations of sales rights and service availability, we cannot guarantee that all products included in this brochure are available through the Siemens Healthineers sales organization worldwide. Availability and packaging may vary by country and are subject to change without prior notice. Some of the features and products described herein may not be available in the United States.

The information in this document contains general technical descriptions of specifications and options as well as standard and optional features which do not always have to be present in individual cases.

Siemens Healthineers reserves the right to modify the design, packaging, specifications, and options described herein without prior notice. Please contact your local Siemens sales representative for the most current information.

Note: Any technical data contained in this document may vary within defined tolerances. Original images always lose a certain amount of detail when reproduced.

International version.
Not for distribution or use in the U.S.

·· .

Siemens Healthineers Headquarters
Siemens Healthcare GmbH
Henkestr. 127
91052 Erlangen, Germany
Phone: +49 9131 84-0
siemens.com/healthineers